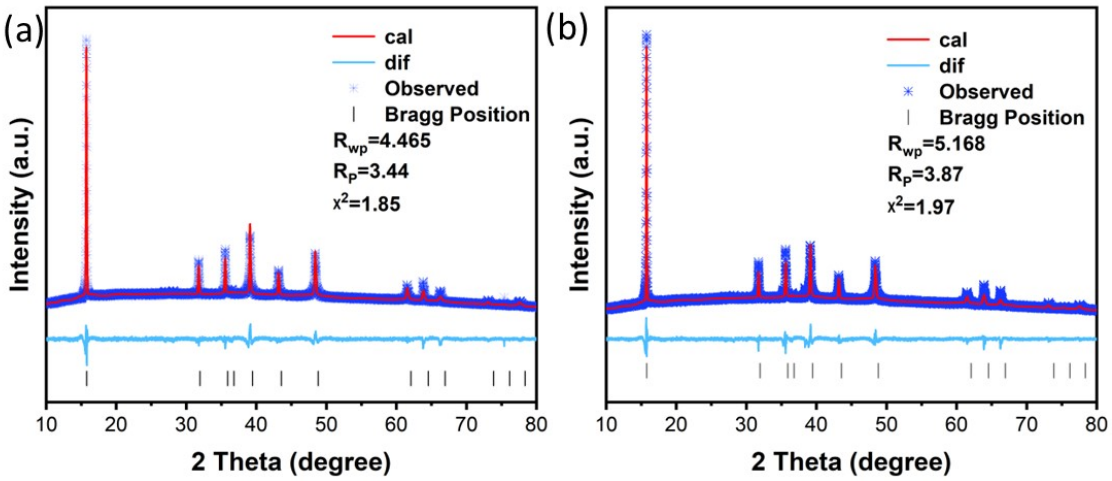

Figure S1. Rietveld refinements of (a) $Na_{0.67}Ni_{0.23}Mn_{0.67}Cu_{0.05}O_2$ and (b) $Na_{0.67}Ni_{0.23}Mn_{0.67}Cu_{0.15}O_2$

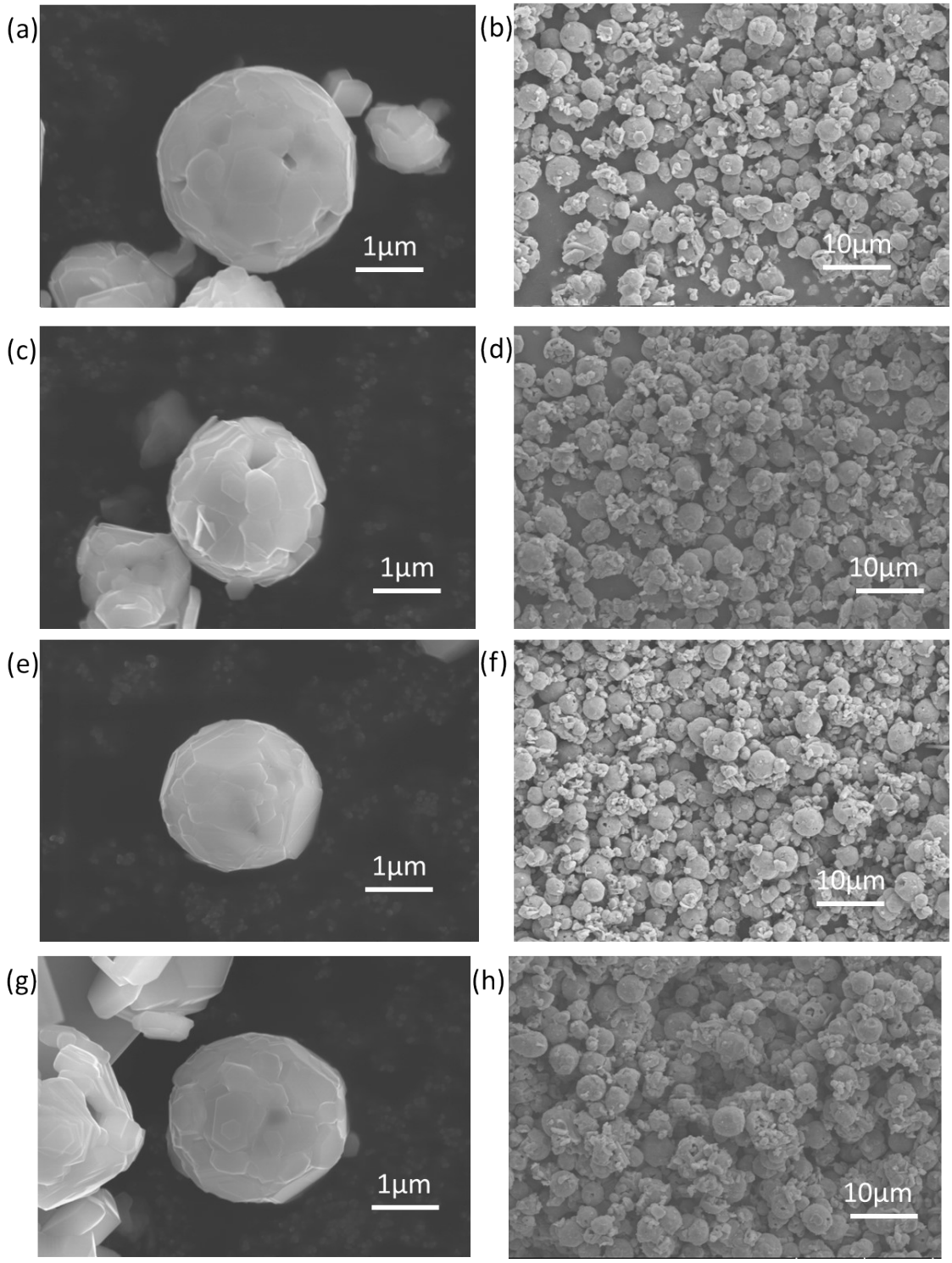

Figure S2. SEM of (a) and (b) $Na_{0.67}Ni_{0.33}Mn_{0.67}O_2$, (c) and (d) $Na_{0.67}Ni_{0.23}Mn_{0.67}Cu_{0.05}O_2$, (e) and (f) $Na_{0.67}Ni_{0.23}Mn_{0.67}Cu_{0.1}O_2$, (g) and (h) $Na_{0.67}Ni_{0.23}Mn_{0.67}Cu_{0.15}O_2$.

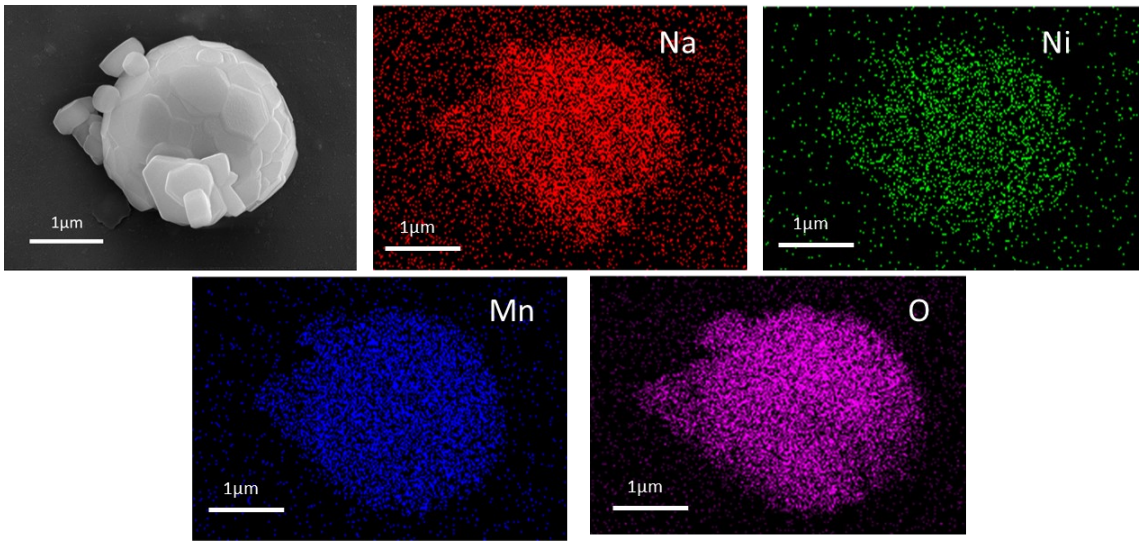

Figure S3. EDS of $Na_{0.67}Ni_{0.33}Mn_{0.67}O_2$

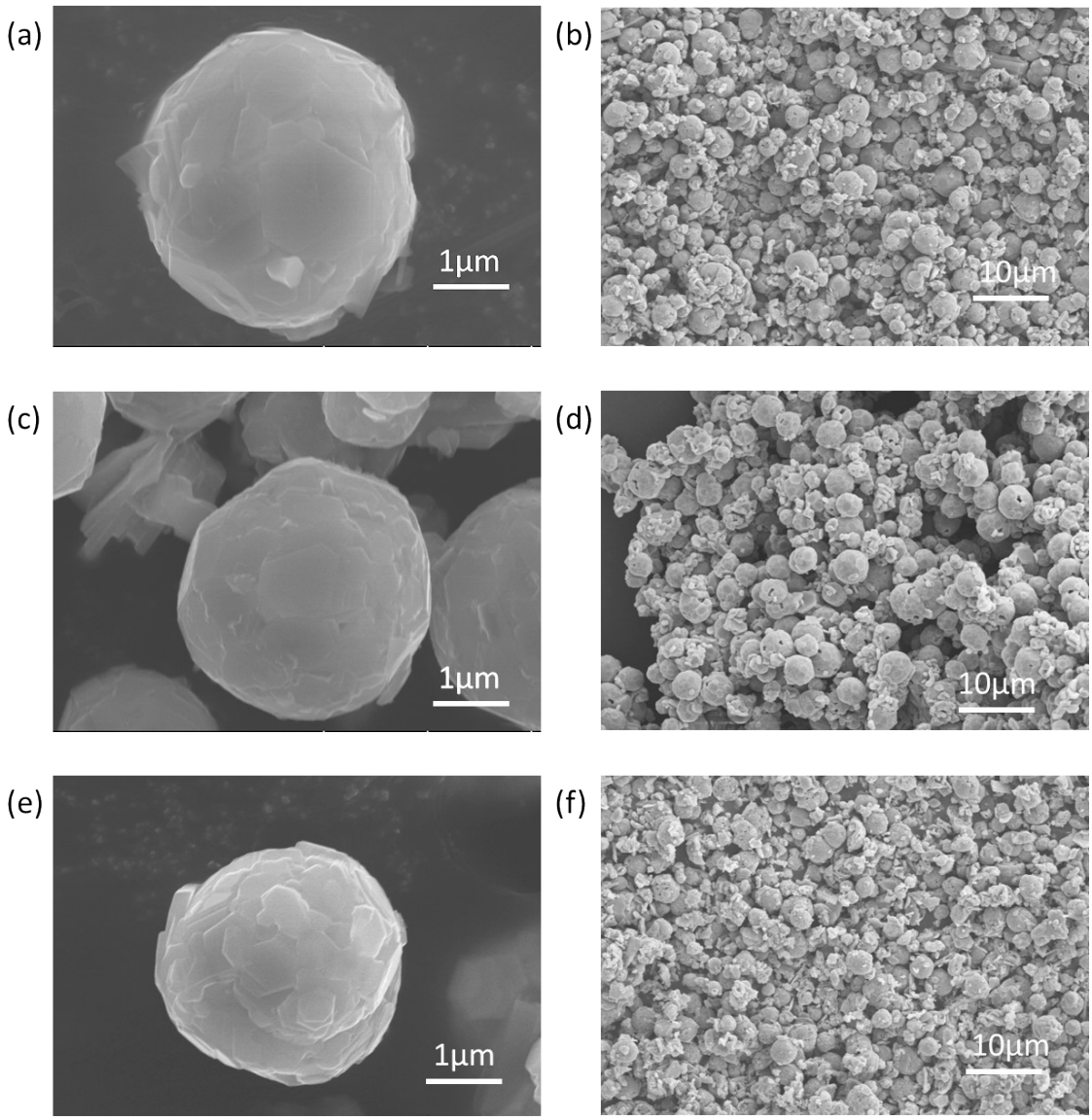

Figure S4. SEM of (a) and (b) $Na_{0.67}Ni_{0.23}Mn_{0.67}Cu_{0.1}O_{0.9}F_{0.05}$, (c) and (d) $Na_{0.67}Ni_{0.23}Mn_{0.67}Cu_{0.1}O_{0.9}F_{0.1}$, (e) and (f) $Na_{0.67}Ni_{0.23}Mn_{0.67}Cu_{0.1}O_{0.85}F_{0.15}$

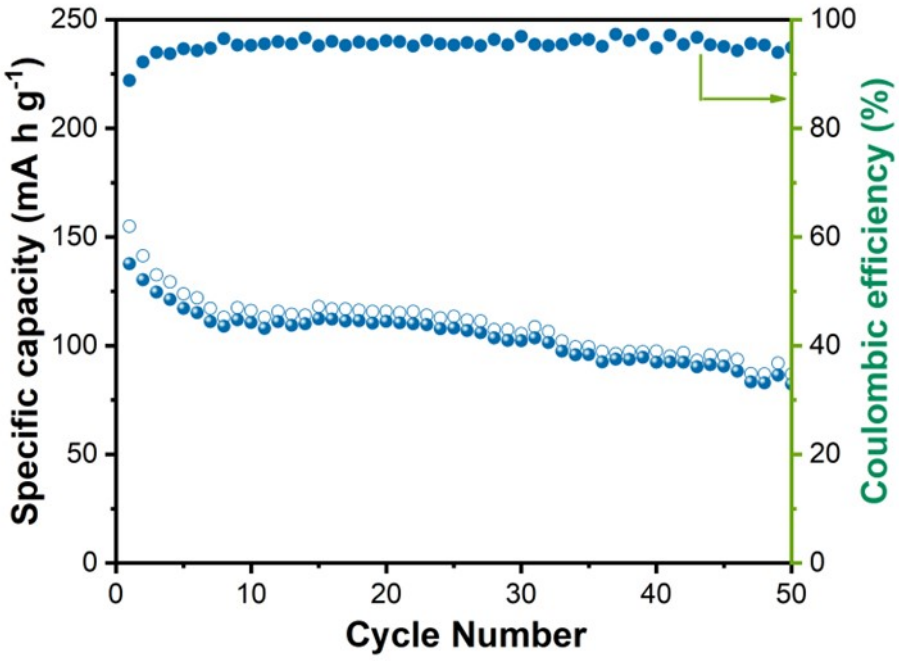

Figure S5. Cycling performance at 0.1 C between 2.0 and 4.4 V of NNM.

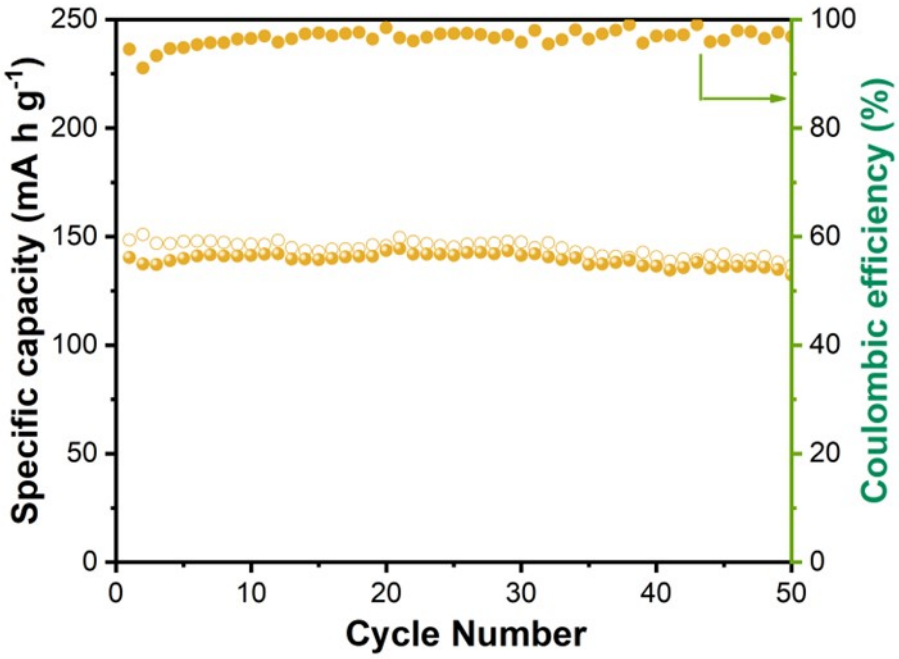

Figure S6. Cycling performance at 0.1 C between 2.0 and 4.4 V of NNMC10F10.

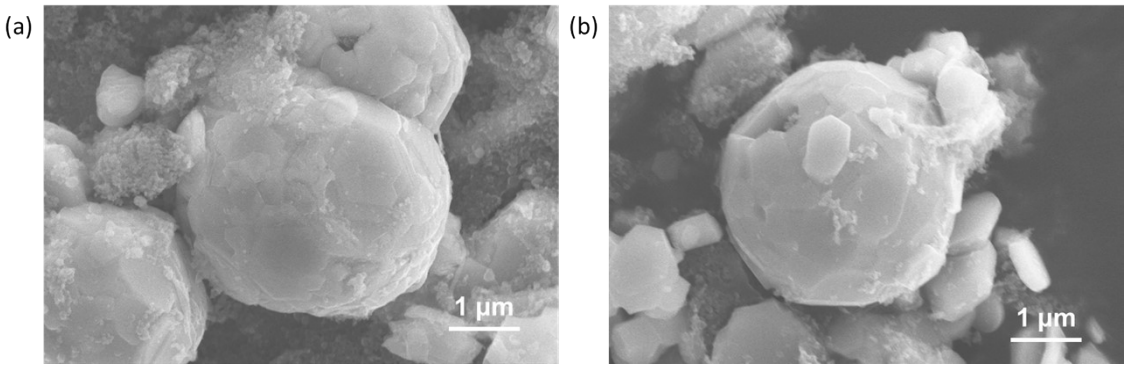

Figure S7. SEM after 100 cycles of (a) NNM and (b) NNMC10F10.

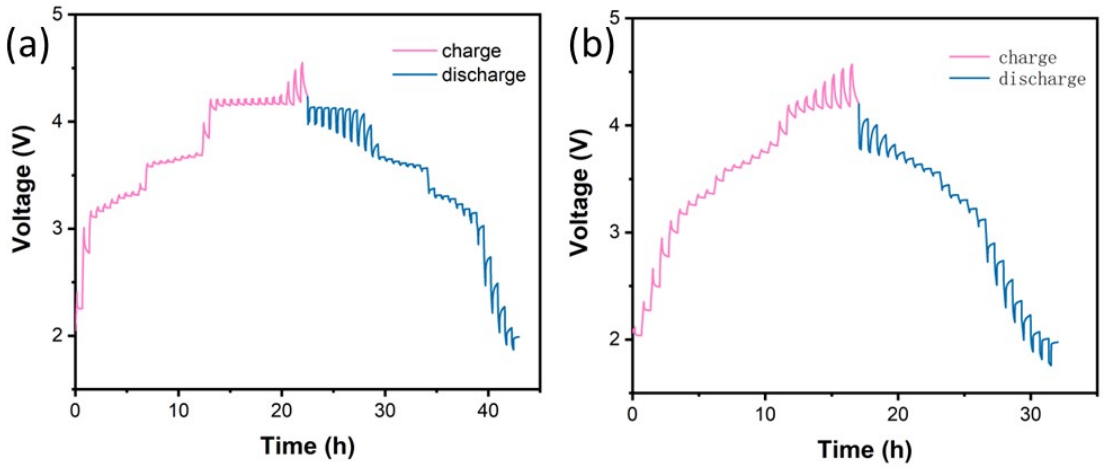

Figure S8. GITT curves of P2-type cathode material (a) NNM and (b) NNMC10F10.

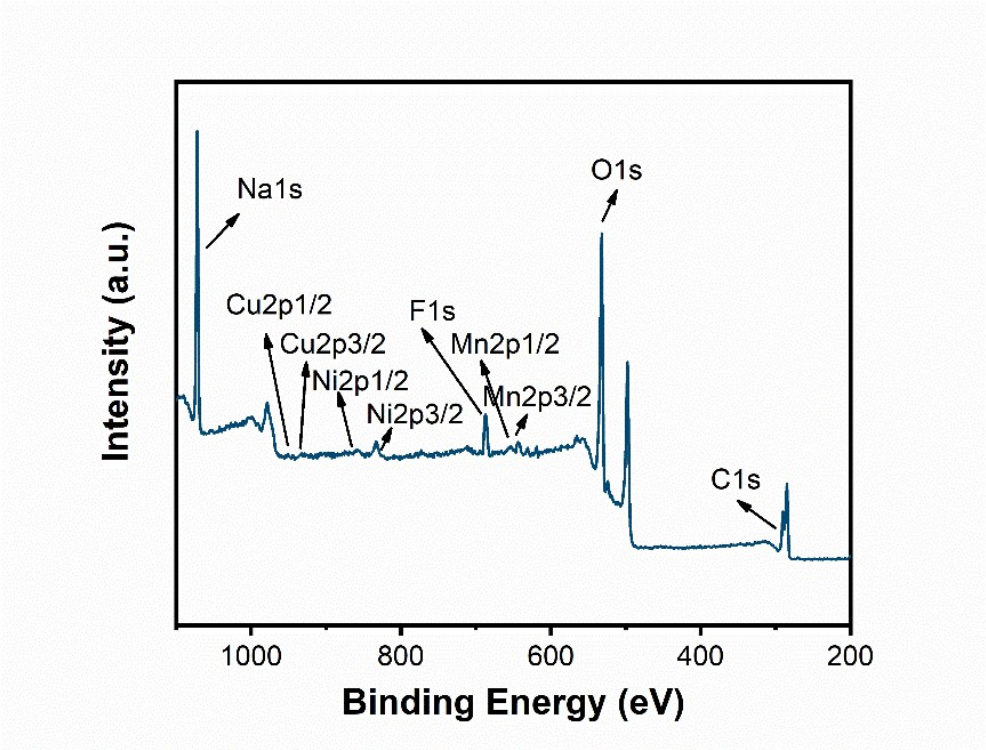

Figure S9. XPS spectrum after the NNMC10F10 cycle.

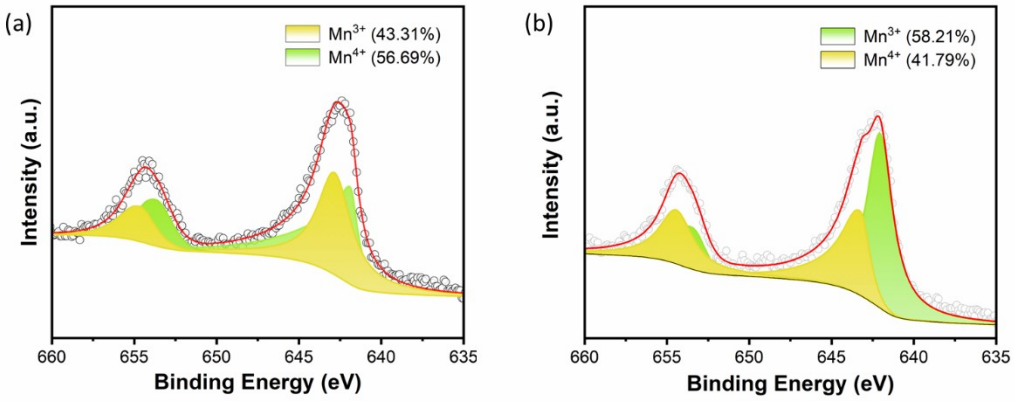

Figure S10. XPS tests of (a) NNM and (b) NNMC10F10 for Mn 2p spectrum.

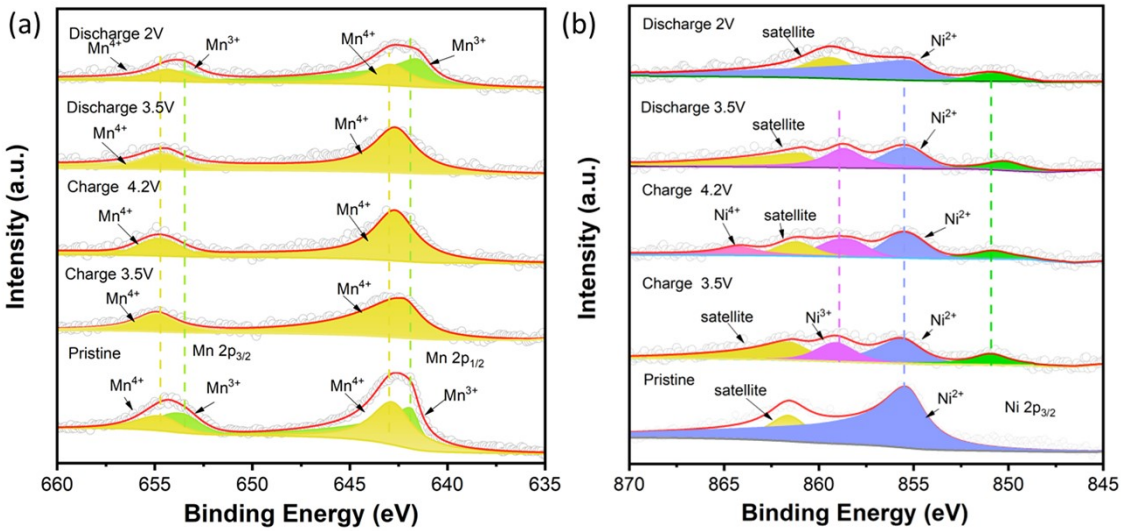

Figure S11. Ex situ XPS tests of NNM for (a) Mn 2p spectrum and (b) Ni 2p spectrum.

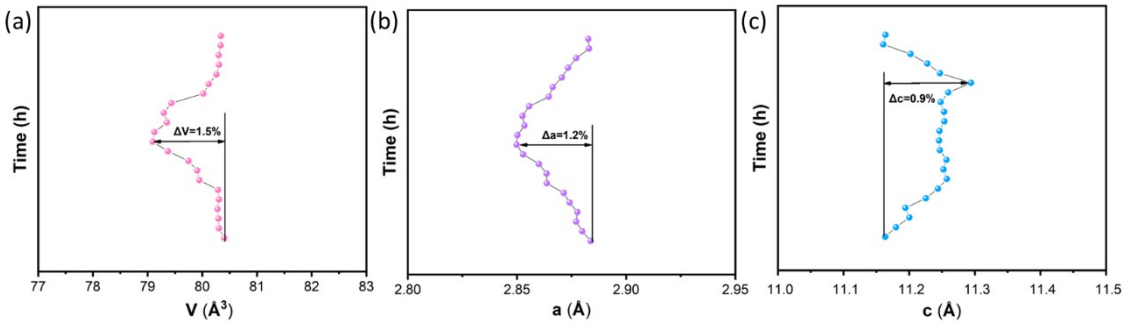

Figure S12. Changes in structural parameters during in-situ XRD testing (a) unit cell volume V, (b) lattice parameter a and (c) lattice parameter c.

Table S1. Detailed structural parameters of the $Na_{0.67}Ni_{0.33-x}Mn_{0.67}Cu_xO_2$ (x=0，0.05，0.1，0.15) samples determined by the XRD Rietveld refinement.

Synthesized samples	a (Å)	c (Å)	V (Å3)	Rwp
x=0	2.90647	11.21019	82.012	4.472%
x=0.05	2.90792	11.22016	82.166	6.742%
x=0.1	2.91355	11.25674	82.754	4.465%
x=0.15	2.91212	11.28198	82.858	5.168%

Table S2. Detailed structural parameters of the $Na_{0.67}Ni_{0.23}Mn_{0.67}Cu_{0.1}O_{2-y}F_y$ (y=0，0.05，0.1，0.15) samples determined by the XRD Rietveld refinement.

Synthesized samples	a (Å)	c (Å)	V (Å3)	Rwp
y=0.05	2.90577	11.22478	82.079	5.52%
y=0.1	2.87360	11.22690	80.287	5.04%
y=0.15	2.91511	11.23157	82.657	6.613%

Table S3. Comparison of BET specific surface areas of the three samples: solid NNM, microsphere NNM, and microsphere NNMC10F10

Thermophysical properties	Solid-phase sample	Sphere NNM	Sphere Cu0.1F0.1
BET Surface Area ($m^2 g^{-1}$)	7.3839	3.5242	0.0985
BJH Adsorption average pore diameter (nm)	6.0066	4.5712	15.3932
BJH Desorption average pore diameter (nm)	6.4153	6.2709	40.0035

Table S4. Comparison of unit cell volume variation between this work and other previously reported sodium layered oxide cathodes.

Sample	Volume change	Reference(s)
P2-$Na_{0.7}Ni_{0.2}Co_{0.2}Mn_{0.5}Fe_{0.1}O_2$	11.90%	1
P2-$Na_{0.67}Ni_{0.18}Mn_{0.67}Cu_{0.1}Zn_{0.05}O_2$	6.96%	2
P2–$Na_{0.66}Li_{0.18}Fe_{0.12}Mn_{0.7}O_2$	3.50%	3
P2-$Na_{0.67}Mn_{0.7}Cu_{0.15}Ti_{0.15}O_2$	3.20%	4
$Na_3V_2(PO_4)_2O_2F$	2.56%	5
P2-$Na_{0.56}Co_{0.17}Mn_{0.8}La_{0.03}O_2$	1.90%	6
P2-$Na_{2/3}Mn_{1/2}Ni_{1/6}Co_{1/3}O_2$	1.90%	7
This work	1.50%	This work

Table S5. The elemental molar ratio of the material was determined through inductively coupled plasma (ICP) analysis.

Sample	Na	Ni	Cu	Mn
$Na_{0.67}Ni_{0.33}Mn_{0.67}O_2$	0.674396	0.328932	□	0.67
$Na_{0.67}Ni_{0.23}Mn_{0.67}Cu_{0.1}O_2$	0.672936	0.237554	0.119647	0.67
$Na_{0.67}Ni_{0.23}Mn_{0.67}Cu_{0.1}O_{1.9}F_{0.1}$	0.662782	0.230833	0.106393	0.67

Table S6. Performance comparison between our work and other reported works.

Sample	Initial capacity (mA g^{-1})	Cycling Retention	Voltage Window (V)	Reference
P2- $Na_{0.66}Li_{0.18}Mn_{0.71}Mg_{0.21}Co_{0.08}O_2$	166	82%, 100 cycle, 20 mA g^{-1}	1.5-4.5	8
P2-$Na_{0.93}Li_{0.07}Cu_{0.07}Ni_{0.29}Mn_{0.57}O_2$	110	85%, 200 cycle, 0.2 C	2.0-4.2	9
O3-Na $[Fe_{1/3}Ni_{1/3}Mn_{1/3}]_{0.95}Cu_{0.05}O_2$	127.2	80.7%, 200 cycle, 0.5 C	2.0-4.0	10
P2-$Na_{0.67}Fe_{0.1}Mn_{0.8}Cu_{0.1}F_{0.1}O_{1.9}$	163.8	80.6%, 100 cycle, 100 mA g^{-1}	1.5-4.5	11
P2-$Na_{2/3}Zn0._{18}Ti_{0.10}Mn_{0.72}O_2$	134	78.2%, 50 cycle, 0.1 C	2.0-4.6	12
O3-$NaMn_{0.48}Fe_{0.32}Cu_{0.2}O_2$	103.76	82.9%, 100 cycle, 24 mA g^{-1}	2.1-4.3	13
P2-$Na_{0.66}Ni_{0.12}Li_{0.05}Cu_{0.10}Mn_{0.72}O_2$	113.5	82.15%, 100cycle, 1 C	2-4.5	14
P2–$Na_{0.6}Ni_{0.2}Mn_{0.7}Cu_{0.1}O_2$	135	76%, 100cycle, 0.1 C	2-4.5	15
P2-$Na_{0.67}Ni_{0.33}Mn_{0.57}Cu_{0.05}Mo_{0.05}O_2$	120	80.2%, 200cycle, 0.5 C	2-4.5	116
P2-$Na_{0.67}Fe_{0.3}Mn_{0.5}Cu_{0.15}Ti_{0.05}O_2$	161.3	77.1%, 100 cycle, 200 mA g^{-1}	1.5-4.3	17
P2- $Na_{0.67}Ni_{0.23}Mn_{0.67}Cu_{0.1}O_{0.9}F_{0.1}$	130.8	88.07%, 100cycle, 1 C	2-4.4	This work

REFERENCES

[1] Jeong S, Kim I, Eom S, Hwang H, Jung Y and Kim J. Engineering the local chemistry through fe substitution in layered P2-$Na_{0.7}Ni_{0.2}Co_{0.2}Mn_{0.6}O_2$ for high-performance Sodium-Ion batteries. Energy Storage Materials 75 (2025) 104041.

[2] Yin S, Tao Z, Zhang Y, Zhang X, Yu L, Ji F, Ma X, Yuan G and Zhang G. Constructing a Size-Controllable Spherical P2-Type Layered Oxides Cathode That Achieves Practicable Sodium-Ion Batteries. ACS Appl. Mater. Interfaces 2024, 16, 20, 26340-26347.

[3] Yang L, Li X, Liu J, Xiong S, Ma X, Liu P, Bai J, Xu W, Tang Y, Hu Y, Liu M and Chen H. Lithium-Doping Stabilized High-Performance P2-$Na_{0.66}Li_{0.18}Fe_{0.12}Mn_{0.7}O_2$ Cathode for Sodium Ion Batteries. J. Am. Chem. Soc. 2019, 141, 16, 6680-6689.

[4] Zhang X, Qiu F, Jiang K, He P, Han M, Gou S and Zhou H. Improving the structural and cyclic stabilities of P2-type $Na_{0.67}MnO_2$ cathode material via Cu and Ti co-substitution for sodium ion batteries. Chem. Commun., 2020, 56,6293.

[5] Gou J, Wang L, Wu X, Zhang X, Yan Q, Chen H, Zhang J and Gou Y. High-Energy/Power and Low-Temperature Cathode for Sodium-Ion Batteries: In Situ XRD Study and Superior Full-Cell Performance. Adv. Mater. 2017, 29, 1701968.

[6] Xia F, Tie D, Wang J, Song H, Wen W, Ye X, Wu J, Hou Y, Lu X and Zhao Y. Ultrahigh rate and durable sodium-ion storage at a wide potential window via lanthanide doping and perovskite surface decoration on layered manganese oxides. Energy Storage Materials 42 (2021) 209-218.

[7] Liu Z, Shen J, Feng S, Huang Y, Wu D, Li F, Zhu Y, Gu M, Liu Q, Liu J and Zhu M. Ultralow Volume Change of P2-Type Layered Oxide Cathode for Na-Ion Batteries with Controlled Phase Transition by Regulating Distribution of Na. Angew. Chem. Int. Ed. 2021, 60, 20960-20969.

[8] Xiao J, Zhang F, Tang K, Li X, Wang D, Wang Y, Liu H, Wu M and Wang G. Rational Design of a P2-Type Spherical Layered Oxide Cathode for High-Performance Sodium-Ion Batteries. ACS Cent. Sci. 2019, 5, 12, 1937-1945.

[9] Anilkumar A, Nair N, Nair S and Baskar S. Tailoring high Na content in P2-type layered oxide cathodes via Cu-Li dual doping for sodium-ion batteries. Journal of Energy Storage 72 (2023) 108291.

[10] Xu X, Liu G, Su C, Zhang Y and Wen L. High stability of Cu-doped O3-type $NaNi_{1/3}Fe_{1/3}Mn_{1/3}O_2$ cathode material for sodium-ion battery. Ionics (2024) 30: 4021-4031.

[11] Zhang Y, Liu G, Su C, Liu G, Sun H, Qiao D and Wen L. Study on the influence of Cu/F dual-doping on the Fe-Mn based compound as cathode material for sodium ion batteries. Journal of Power Sources 536 (2022) 231511.

[12] Chen C, Zhao C, Liu H, Wu X, Hu B, Li J, Hu B and Li C. Mitigating the Formation of Tetrahedral Zn in Layered Oxides Enables Reversible Lattice Oxygen Redox Triggering by the Na-O-Zn Configuration. ACS Nano 2023, 17, 12, 11406-11413.

[13] Zhang Z, Liu Y, Liu Z, Li H, Huang Y, Liu W, Ruan D, Cai X and Yu X. Dual-strategy of Cu-doping and O3 biphasic structure enables Fe/Mn-based layered oxide for high-performance sodium-ion batteries cathode. Journal of Power Sources 567 (2023) 232930.

[14] Yu H, Yu M, Zheng Z, Ma H, Wang J, Zhang Z, Li C, Guo H, Zhang Y and Dong P. Li and Cu double-doped P2-type sodium-ion layered oxide cathode materials with enhanced high-voltage stability. Journal of Alloys and Compounds 1020 (2025) 179425.

[15] Jiang J, He H, Cheng C, Yan T, Xia X, Ding M, He L. Chan T and Zhang L. Improving Structural and Moisture Stability of P2-Layered Cathode Materials for Sodium-Ion Batteries. ACS Appl. Energy Mater. 2022, 5, 1, 1252-1261.

[16] Xue L, Wang J, Teng Y, Lu J and Shuo B. Enhancing the electrochemical performance of P2-type layered cathode by Cu/Mo co-substitution. Materials Letters 303 (2021) 130507.

[17] Li Y, Feng A, Yang T, Chen N, Li A, Yang Y, Liu R, Zhang L and Qin X. Enhanced stability in a layered P2-$Na_{0.67}Fe_{0.5}Mn_{0.5}O_2$ cathode for sodium ion batteries via a synergistic Cu/Ti co-doping strategy. Inorg. Chem. Front., 2025,12,

7250-7260.